

Improving the Validity of Decision Trees as Explanations

Jiri Nemecek, Tomas Pevny, and Jakub Marecek

Department of Computer Science
Czech Technical University in Prague
contact@nemecekjiri.cz

June 14, 2023

Abstract

In classification and forecasting with tabular data, one often utilizes tree-based models. This can be competitive with deep neural networks on tabular data [cf. Grinsztajn *et al.*, NeurIPS 2022] and, under some conditions, explainable. The explainability depends on the depth of the tree and the accuracy in each leaf of the tree. Here, we train a low-depth tree with the objective of minimising the maximum misclassification error across each leaf node, and then “suspend” further tree-based models (e.g., trees of unlimited depth) from each leaf of the low-depth tree. The low-depth tree is easily explainable, while the overall statistical performance of the combined low-depth and suspended tree-based models improves upon decision trees of unlimited depth trained using classical methods (e.g., CART) and is comparable to state-of-the-art methods (e.g., well-tuned XGBoost).

1 Introduction

In classification and forecasting with tabular data, one often utilizes axis-aligned decision trees [1, 2]. A prime example of a high-risk application of AI, where decision trees are widely used, is credit risk scoring [3, 4, 5] in the financial services industry [6]. There, the relevant regulation, such as the Equal Credit Opportunity Act in the US [7] and related regulation [8, 9] in the European Union, bars the use of models that are not explainable [10], which is often construed [11, 12, 13, 14] as requiring the use of decision trees. When studying the decision tree that a bank uses, one often focuses on ways that would make it possible to obtain a loan, and one would wish that the corresponding leaf of the decision tree had as high accuracy as possible.

In many other domains, the use of tree-based models has an equally long tradition. Consider, for example, judicial applications of AI such as the infamous

Correctional Offender Management Profiling for Alternative Sanctions (COMPAS) [15, 16, 17, 18], which is marketed as the “nationally recognized decision tree model”, or medical applications of AI [19, 20, 21, e.g.]. It is hard to overstate the importance of high accuracy of any rule that a medical doctor or a judge may learn from a decision tree. In yet more domains, low-depth decision trees are used [22] to provide globally valid explanations of black-box classifiers, which is sometimes known [22] as model extraction.

Low-depth trees can indeed serve as global explanations for a classifier, or explainable classifiers *per se*, when each leaf is construed as a logical rule. Because various individuals or subgroups may deem various outcomes of importance, cf. the medical applications, a *fair explanation* would have as high accuracy in each leaf of the decision tree as possible. The depth needs to be low¹, in order for the rule explaining the decision in each leaf to remain comprehensible.

Similarly, one could argue that a decision tree can provide misleading explanations. To evaluate how valid² or misleading the decision tree is, we suggest considering the minimal accuracy in any leaf of a tree (tree’s *leaf accuracy*). Indeed, a member of the public, when presented with the decision tree, may assume that each leaf of a decision tree can be construed as a logical rule. Consider, for example, the decision tree of Figure 1, based on the two-year variant of the well-known COMPAS [15] dataset, which considers the binary classification problem of whether the individual would reoffend within the next two years. The left-most leaf may be interpreted as suggesting that for 1-3 prior counts and under 23 years of age, the defendant will not reoffend within the next two years after release. However, the validity of this rule is rather questionable: the training accuracy in that leaf is 66.8 %, while the test accuracy is 60 % in that leaf. This suggests that 40 % defendants who meet these criteria will actually reoffend within two years. For a more extreme example, see Figure 2, which shows two trees of similar overall accuracy for the pol(e) dataset. When optimizing for overall accuracy, the minimum test accuracy in one leaf can be as low as 57.1% (cf. the top tree in Figure 2). However, when maximizing the minimum training accuracy in one leaf, the minimum test accuracy in one leaf increases to 86.5% (cf. the bottom tree in Figure 2). One could argue that this improves the validity and fairness of the explanation provided by the tree.

Although a recent comparison of the statistical performance of gradient-boosted trees and deep neural networks [27] by Grinsztajn *et al.* has shown that the state-of-the-art tree-based models can outperform state-of-the-art neural networks, across a comprehensive benchmark of tabular data sets, the low depth limits the overall accuracy. Therefore, one would like to improve the accuracy by “hybridizing” the tree, where the top, fixed-depth tree maximizing the minimum leaf accuracy objective would explain as much of the variance as possible, given the depth, while below, tree-based models suspended from all leaves of the fixed-

¹According to [23], humans can understand logical rules with boolean complexity of up to 5–9, depending on their ability, where the boolean complexity is the length of the shortest Boolean formula logically equivalent to the concept, usually expressed in terms of the number of literals.

²Our use of the term *validity* is related to its use in [24, 25, 26], but distinct.

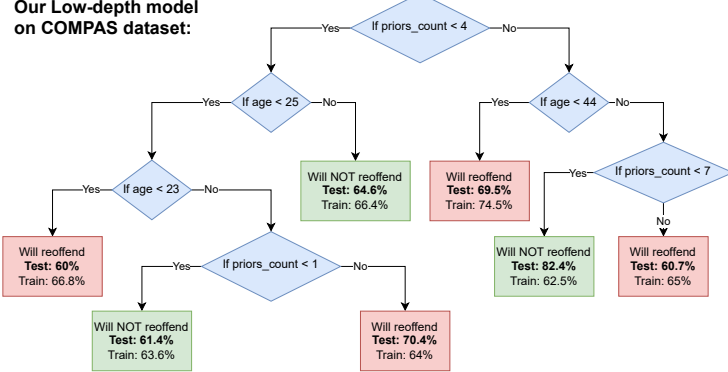


Figure 1: An example of the decision tree produced by our model for the COMPAS dataset, cf. Figure 3. The bold percentage shows the leaf accuracy in each leaf on out-of-sample data, before applying the extending model. Below that, in regular font, we provide accuracy on training data.

depth tree, need not be interpretable, but would improve the overall accuracy of the hybrid tree.

Here, we aim to introduce such hybrid trees and a two-step procedure for training these, to improve upon both the statistical performance and explainability of decision trees. In the first step of the procedure, we use mixed-integer programming (MIP) to train a low-depth tree, with the objective of minimizing the maximum misclassification error across each leaf node, and with constraints bounding the number of samples in each leaf node from below. Seen another way, we maximize the minimal accuracy in any leaf of a tree. In the second step, we train further tree-based models, which are to be suspended from each leaf of the low-depth tree. The low-depth tree with the additional constraints on the accuracy in the leaves is easily explainable, while the overall statistical performance of these hybrid trees [28] combining low-depth trees and suspended tree-based models (which we call the *hybrid-tree accuracy*) improves upon the accuracy of decision trees of unlimited depth trained using classical methods (e.g., CART) and is comparable to state-of-the-art tree-based methods, such as the well-tuned XGBoost of [27].

Let us illustrate the statistical performance. Figure 3 shows that the accuracy of well-tuned gradient-boosted trees of [27] on the two-year COMPAS [15] test case exceeds 0.68. The accuracy of our low-depth tree trained with the leaf-accuracy objective is below 0.65, which should not be surprising, considering the mean accuracy is *not* the main objective. Nevertheless, by utilising the trees suspended from leaf nodes of the low-depth tree, we can improve the accuracy very close to 0.68, which improves over both the accuracy of CART of the same depth alone (0.67) and CART of the same depth with trees suspended from leaf nodes of the CART tree (around 0.675). This performance is rather typical across the benchmark of [27], with the average improvement of 0.0053 on categorical

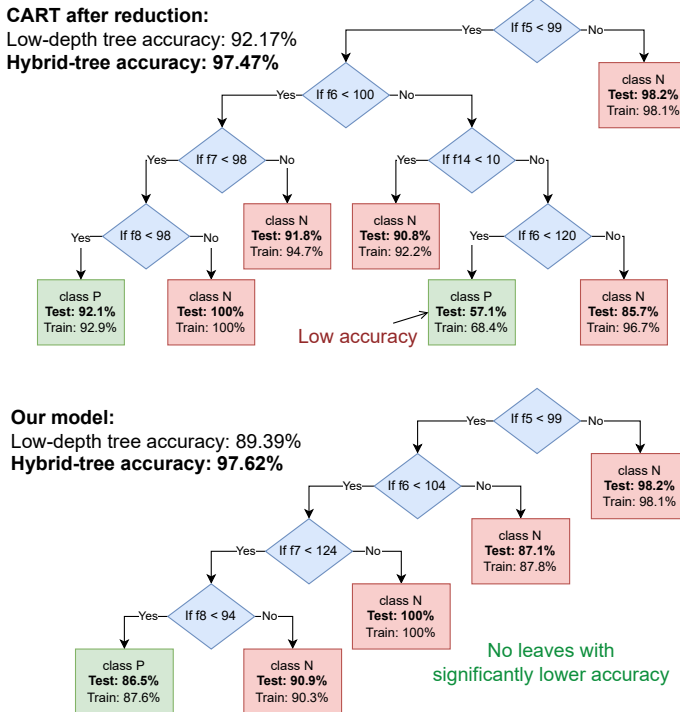


Figure 2: An example of the decision tree produced by our model for *pol* dataset. In each leaf, bold/regular percentage shows the leaf accuracy, before suspending any further tree from it, on the test/training data set, respectively. Below the name of the model, we present the the (hybrid-tree) accuracy of the hybrid/low-depth tree in bold/regular font.

datasets and 0.0016 on numerical datasets over the limited-depth CART tree with further CART trees suspended from its leaves.

Our contributions. We present:

- the challenge of *fairness* (or, equivalently, *validity*) of an explanation.
- leaf accuracy as a criterion for evaluating the validity and fairness of a classification tree as a global explanation.
- a method for training decision trees that are optimal with respect to leaf accuracy, which is scalable across a well-known benchmark [27], despite its use of mixed-integer programming.
- benchmarking on tabular datasets [27] suggesting that the leaf accuracy can be improved by up to 21.16 percentage points (i.e., by 44.84%), while suffering only a very modest drop (at most 2.76 percentage points across the benchmark) in the overall accuracy, compared to well-tuned XGBoost [27].

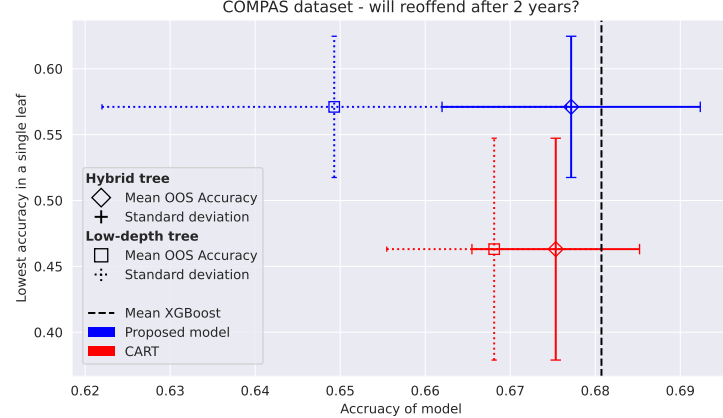


Figure 3: Performance on the COMPAS dataset: Mean statistical performance over 10 different train-test splits, evaluated in terms of accuracy (horizontal axis) and leaf accuracy (vertical axis) for five variants of (hybrid) decision trees. The horizontal and vertical error bars are standard deviations across the 10-fold cross-validation. Notice that the proposed model has better interpretability compared to any standard decision tree and accuracy comparable to a gradient-boosted tree.

2 Related Work

Decision trees [2] are among the leading supervised machine learning methods, where interpretability and out-of-sample classification performance is important. Random forests [29] and gradient-boosting tree-ensemble approaches [30, 31] improve upon their statistical performance substantially, while limiting the interpretability, somewhat. We are given n samples $(x_{i1}, \dots, x_{ip}, y_i)$ with p features each, for $i = 1 \dots n$, and their classification $y_i \in [K]$ into K classes. Let us denote sample i by $\mathbf{x}_i = (x_{i1}, \dots, x_{ip})$. The decision trees sequentially splits the samples into subsamples: In each non-leaf node t , it splits the samples based on a single covariate $x_{:t}$ and a threshold b_t . (See Figure 1 for an illustration.) There is a vast literature, including the construction of confidence intervals [32]. More recently, decision trees play an important role in explainable artificial intelligence [33, 34] and interpretable machine learning [35].

Construction of a optimal axis-aligned binary decision tree is NP-Hard [36], and there are hence cases when all known polynomial-time algorithms such as CART [2] produce suboptimal results. Still, CART [2], which utilizes Gini diversity index and cross-validation in pruning trees, ranks among the leading algorithms [37] in machine learning. A decade later, Breiman suggested that boosting can be interpreted as an optimization algorithm [38], leading to the development of gradient-boosted trees [30, 31, e.g.]. Their well-tuned variants [39, 40, 41, e.g.,] are the state-of-the-art polynomial-time algorithms for training decision trees. We refer to [42, 27] for comparisons against deep neural networks.

Bertsimas and Dunn [43] and, independently others [44, 45, 46], pioneered the use of exponential-time algorithms in the construction of decision trees, under the banner of *optimal decision trees*. The integer-programming formulation of [43] suffers from some issues of scalability [47], but can be easily extended by the addition of further constraints, such as sparsity [48, 49, 50], fairness [47, 51], upper bounds on the numbers of leaves [52], incremental progress bounds [52], bounds on similarity of the support [52], a wide variety of privacy-related constraints, and in our case, numbers of samples and accuracy in the leaves. Likewise, there are numerous extensions in terms of the objective [52], including F-score, AUC, and partial area under the ROC convex hull, and in our case, the minimum leaf accuracy. Subsequently, the *optimal decision trees* have grown into a substantial subfield within machine learning research.

There have been a number of important proposals as to alternative convex-programming relaxations for optimal decision trees: [53] have demonstrated the use of an extended formulation in a column-generation (branch-and-price) approach; [54] have introduced another alternative formulation and a number of valid inequalities (cuts); [55] have introduced yet another alternative formulation based on the maximum-flow problem. [52]. Independently, [56] suggested to use non-linear optimization techniques, such as alternating minimization leading to a much further research [57]. We refer to [58, 59] for overviews of mathematical optimization in the construction of decision trees.

Much recent research [60, 61, 51, 62, 63, e.g.] has also focussed on improving the scalability of exponential-time algorithms for optimal decision trees by using branch-and-bound methods without relaxations in the form of convex optimization and, more broadly, dynamic programming. These approaches are sometimes seen as less transparent, as the mixed-integer formulation needs to be translated to the appropriate pruning rules or cost-to-go functions, which are less succinct, and the correctness of the translation can be non-trivial to verify. Nevertheless, [62] have demonstrated the scalability of their method to a dataset with over 245,000 samples (utilizing less than 2000 core-hours), for example. On a benchmark of 21 datasets from UCI Repository with over 7,000 samples, the algorithm can improve training accuracy by 3.6% and testing accuracy by 2.8%, compared to the current state-of-the-art. This seems to validate the practical relevance of optimal decision trees.

3 Mixed-Integer Formulation

We extend the Mixed-Integer Programming (MIP) formulation of *optimal decision trees* [43] to a different objective function and novel constraints. The entire MIP formulation is presented in Figure 4.

Base model As in the original optimal decision trees [43], we have n samples with p features each. Every point has one of K classes, which is represented in the formulation by a binary matrix Y such that $Y_{ik} = 1 \iff y_i = k$. All tree nodes are split into two disjoint sets \mathcal{T}_B and \mathcal{T}_L which are sets of branching

$$\begin{aligned}
& \max Q && (1) \\
\text{s. t. } & Q \leq \sum_{i=1}^n S_{it} + (1 - l_t) && \forall t \in \mathcal{T}_L && (2) \\
& s_{it} \leq z_{it} && \forall i \in \{1, \dots, n\}, \quad \forall t \in \mathcal{T}_L && (3) \\
& r_t \leq s_{it} + (1 - z_{it}) && \forall i \in \{1, \dots, n\}, \quad \forall t \in \mathcal{T}_L && (4) \\
& r_t \geq s_{it} + (z_{it} - 1) && \forall i \in \{1, \dots, n\}, \quad \forall t \in \mathcal{T}_L && (5) \\
& l_t = \sum_{i=1}^n s_{it} && \forall t \in \mathcal{T}_L && (6) \\
& S_{it} \leq s_{it} && \forall i \in \{1, \dots, n\}, \quad \forall t \in \mathcal{T}_L && (7) \\
& S_{it} \leq \sum_{k=1}^K Y_{ik} c_{kt} && \forall i \in \{1, \dots, n\}, \quad \forall t \in \mathcal{T}_L && (8) \\
& S_{it} \geq s_{it} + \sum_{k=1}^K Y_{ik} c_{kt} - 1 && \forall i \in \{1, \dots, n\}, \quad \forall t \in \mathcal{T}_L && (9) \\
& l_t = \sum_{k=1}^K c_{kt} && \forall t \in \mathcal{T}_L && (10) \\
& \mathbf{a}_m^\top \mathbf{x}_i \geq b_m - (1 - z_{it}) && \forall i \in \{1, \dots, n\}, \forall t \in \mathcal{T}_L, \forall m \in A_R(t) && (11) \\
& \mathbf{a}_m^\top (\mathbf{x}_i + \boldsymbol{\epsilon}) \leq && && (12) \\
& b_m + (1 + \epsilon_{\max})(1 - z_{it}) && \forall i \in \{1, \dots, n\}, \forall t \in \mathcal{T}_L, \forall m \in A_L(t) && (13) \\
& \sum_{t \in \mathcal{T}_L} z_{it} = 1 && \forall i \in \{1, \dots, n\} && (14) \\
& z_{it} \leq l_t && \forall i \in \{1, \dots, n\}, \quad \forall t \in \mathcal{T}_L && (15) \\
& \sum_{i=1}^n z_{it} \geq N_{\min} l_t && \forall t \in \mathcal{T}_L && (16) \\
& \sum_{j=1}^p a_{jt} = 1 && \forall t \in \mathcal{T}_B && (17) \\
& 0 \leq b_t \leq 1 && \forall t \in \mathcal{T}_B && (18) \\
& z_{it}, l_t \in \{0, 1\} && \forall i \in \{1, \dots, n\}, \quad \forall t \in \mathcal{T}_L && (19) \\
& a_{jt} \in \{0, 1\} && \forall j \in \{1, \dots, p\}, \quad \forall t \in \mathcal{T}_B && (20) \\
& c_{kt} \in \{0, 1\} && \forall k \in \{1, \dots, K\}, \quad \forall t \in \mathcal{T}_L && (21) \\
& 0 \leq Q, r_t, S_{it}, s_{it} \leq 1 && \forall i \in \{1, \dots, n\}, \quad \forall t \in \mathcal{T}_L && (22)
\end{aligned}$$

Figure 4: The complete formulation of training the low-depth tree maximising the minimum accuracy across all leaf nodes, and constraining the number of samples per leaf node. The constraints in black type are the optimal decision trees of Bertsimas et al. [43], whereas the constraints and variables in violet are our extension.

nodes and leaf nodes respectively. Variable \mathbf{a}_t is a binary vector of dimension p , that selects a variable to be used for decisions in node t . b_t is then the value of the threshold. We assume all data are normalized to $[0, 1]$ range.

Equations (10–21) capture the original model of [43], wherein:

- Binary variable c_{kt} is equal to 1 if and only if leaf node t assigns class k to data.
- Binary variable l_t is equal to 1 if and only if there is any point classified by the leaf node t .
- Binary variable z_{it} is equal to 1 if and only if point x_i is classified by leaf node t .

The only modification to the original formulation is the omission a binary variable d_t that decided whether a certain branching node is used. This introduced a flaw in the original formulation [43] which lead to invalid trees, so we decided against using it. We assume it to always be 1 instead. To prune redundancies, we introduce a process of tree reduction described in Section 3.

Equations (11) and (13) implement the split of samples to leaf node t using disjoint sets $A_R(t)$ and $A_L(t)$, containing nodes to which the leaf t is on the right or on the left, respectively. Since we cannot use strict inequality, we use ϵ , a p -dimension vector of the smallest increments between two distinct consecutive values in every feature space [43]:

$$\epsilon_j = \min \left\{ x_j^{(i+1)} - x_j^{(i)} \mid x_j^{(i+1)} \neq x_j^{(i)}, \forall i \in \{1, \dots, n-1\} \right\}$$

where $x_j^{(i)}$ is the i -th largest value in the j -th feature. ϵ_{\max} is the highest value of ϵ_j and serves as a tight big-M bound.

Finally, Equation (16) bounds the minimal number of points (N_{\min}) in a single leaf from below, similar to [52].

Extensions In the original optimal decision trees [43], the objective is to minimize total misclassification error. Instead, we wish to maximize the minimum leaf accuracy. Because a single sample usually contributes differently to accuracy at different leaves, we need to introduce multiple new variables to track the accuracy in each leaf:

- variable s_{it} represents the potential accuracy that a sample x_i has in leaf t . It takes values in the range $[0, 1]$ and must sum to 1 when summing across all samples assigned to leaf t . This is ensured by setting the value to 0 for all points that are not assigned to the leaf t in Constraint (3). The sum of 1 is enforced in Equation (6) for leaves with some samples assigned. Empty leaves do not have non-zero s_{it} values for any i , and would thus not sum to 1.
- reference accuracy variable r_t serves as a common variable to which all accuracy contributions are equal. This is, of course, required only for points assigned to the leaf t . This is enforced in (4) and (5).

- variable S_{it} represents the true assignment of accuracy given by the sample. That is achieved by setting it to 0 for misclassified points using constraint (8) and by setting it equal to s_{it} otherwise by constraints (7) and (9).
- variable Q is our objective and represents the lowest achieved accuracy across all non-empty leaves as per constraint (2). For empty leaves, this constraint will be trivially satisfied, since Q cannot take value higher than 1 anyway.

Tree reduction After the optimizer of the mixed-integer program is obtained, empty leaves are pruned to obtain the resulting unbalanced tree. Furthermore, to account for suboptimal solutions obtained when the solver is run with a strict time limit, each pair of sibling leaves classified in the same class is merged. This is performed recursively until no further action can be performed. This leads to no loss in total accuracy, and oftentimes leads to an improvement in leaf accuracy, given the fact that we consider the minimum over all leaves.

Tree extension Finally, we suspend new tree-based models from the remaining leaves, to improve hybrid-tree accuracy that is comparable to the best-performing models. In particular, we used XGBoost to train the suspended models, since it was the best-performing model on the benchmark [27]. We trained a separate model for each leaf of the low-depth tree obtained in Section 3 above. The hyperparameters of the models were tuned using 50 iterations of a Bayesian hyperparameter search with 3-fold cross-validation in each leaf. In experiments, we extend trees generated by other methods (OCT, CART) in the same way.

4 Numerical results

We have implemented the method in Python and all code and results are provided in the Supplementary material. We will release them under an open-source license on GitHub once the paper has been accepted. The hyperparameters have been chosen as follows:

- The low-depth trees have been trained using the formulation in Figure 4 with depth limited to four since that is a reasonable threshold for interpretability (e.g., printability on an A4 page, similar to Figure 1) and for not diluting the dataset to small parts that would impede the ability to train the “suspended” trees.
- To further support this, we set the minimal amount of points in a leaf (N_{\min}) to 50.
- MIPFocus and Heuristics hyperparameters were set to 1 and 0.8, respectively, to focus on finding feasible solutions in the search since that leads to the fastest improvements of the solution. However, our experiments in Appendix A.3.1 show that default MIP solver hyperparameters perform similarly.

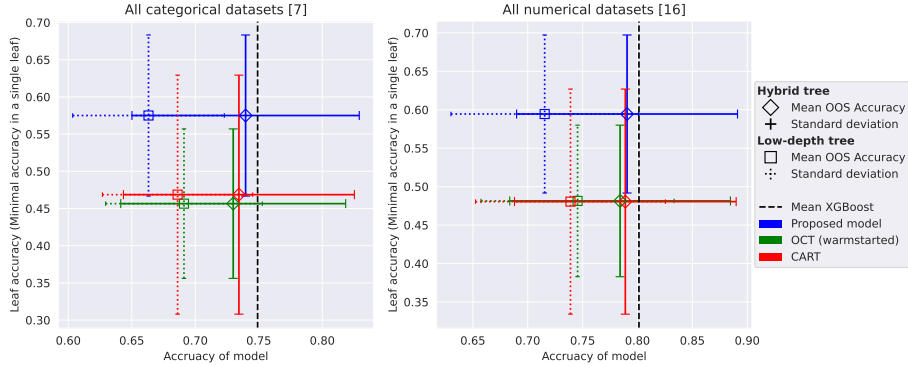


Figure 5: Results on out-of-sample data. The plot shows a significant increase in leaf accuracy when using our method, significantly improving the validity of the explanations provided. It also shows an increase in total accuracy when extending the model with XGBoost models in leaves. Results of the OCT model (warmstarted by the same initial model as the Proposed model) serve to compare to the model we extended.

We performed our experiments on the benchmark dataset of Grinsztajn et al. [27], which contains datasets for both regression and classification. Since our implementation considers only classification, for the time being, we consider only classification datasets. [27] divides the datasets into numerical datasets and datasets with some categorical features. We follow this distinction and present results on both kinds of datasets separately. We also follow the suggestion of [27] to perform 10 different train-test splits with at most 10,000 datapoints or 80% of total datapoints (whichever is lower) for training across all datasets. That is, each model has been trained on each dataset 10 times, with different seeds for data splits. The training used 80% of all data points data or 10,000 datapoints, whichever is lower, while the remaining 20% of the dataset has been used as the test set for evaluating the accuracy, and minimum leaf accuracy Q (2). All MIP formulations of our low-depth tree were warmstarted using a CART solution trained on the same data with default scikit-learn parameters, except maximal depth and a minimal number of samples in a leaf, which were set to 4 and 50, respectively.

We performed all experiments on an internal cluster with sufficient amounts of memory. Each run of the MIP solver has been limited to 8 hours on 8 cores of AMD Epyc 7543, totaling 64 core-hours per split of a dataset. The extension part takes on average around 1 additional 3 core-hours per split. This totals around 15,500 core-hours for the entire classification part of the benchmark of [27] and one configuration of hyperparameters. Training each dataset requires between 15 and 95 GB of working memory; details are provided in the Appendix (Figure 9).

We compare our method of training classification trees to CART, as it is by far

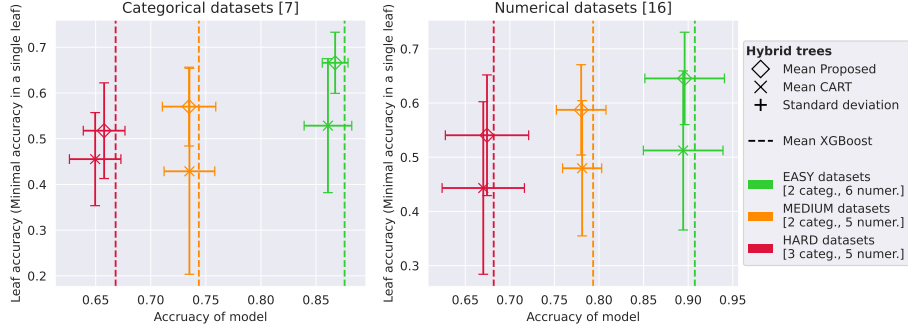


Figure 6: Results on out-of-sample data on all classification datasets from the tabular benchmark. In square brackets are the numbers of datasets belonging to each set. This plot shows that our method, when extended in leaves, does not significantly decrease overall performance compared to pure XGBoost while sometimes improving upon accuracy obtainable by extended CART.

the most common. All experiments used the scikit-learn implementation of CART. The hyperparameters for CART were optimized using Bayesian hyperparameter optimization for 100 iterations using 5-fold cross-validation. Hyperparameter search space was notably constrained only by a maximal depth of 4 to ensure comparability to our low-depth trees. In comparison to unconstrained depth CART, our model interestingly performed even better. See Appendix A.9.1. The entire optimization of CART with the extensions of the leaves took around 500 core-hours for the entire benchmark. The XGBoost results are taken from the authors of the paper [27] introducing the benchmark datasets, which suggests 20,000 core-hours have been spent producing these.

Figure 5 shows the average performance (accuracy and minimum leaf accuracy) over categorical and numerical datasets. We include the comparison to optimal classification trees (OCT) [43] since it is the formulation we built on. The OCT models are warmstarted by the same trees as Our models. The performance of OCT is similar to CART. Our model improves the minimal leaf accuracy by 11.16 percentage points on average compared to CART.

Figure 6 shows again the average performance separately on Categorical and Numerical datasets divided into three groups by difficulty. The measure of difficulty is based on performance by XGBoost provided by the authors of the benchmark. The thresholds of difficulty categories are 0.7 and 0.8 for datasets containing categorical features and 0.75 and 0.85 for datasets with only numerical features. The thresholds were selected in order to separate too easy and too hard datasets, which make the plots less informative, and to explore behavior over datasets with varying inner complexity. We see that the proposed method always significantly improves the minimum leaf accuracy and also improves the accuracy compared to CART.

Table 1 quantifies the differences numerically. Our model have worse accuracy

Table 1: Improvements of mean accuracy on datasets between our model and comparable models. Data is computed by subtracting the mean accuracy of CART or XGBoost, respectively, on each dataset from the mean accuracy of our model. In the first two rows, we compare the leaf accuracy of our model to CART. In the middle two rows, we compare the model accuracy of the hybrid trees with CART extended in the same way. In the last two rows, we compare our extended hybrid-tree model to the mean XGBoost model trained on the same dataset.

	Data type	Min	Mean (\pm std)	Max
<i>Compared to CART</i>				
Leaf Accuracy	categorical	−0.0247	0.1064 \pm 0.0729	0.1905
	numerical	−0.0553	0.1139 \pm 0.0630	0.2116
Hybrid-tree Acc.	categorical	−0.0027	0.0053 \pm 0.0084	0.0182
	numerical	−0.0253	0.0016 \pm 0.0086	0.0111
<i>Compared to XGBoost</i>				
Hybrid-tree Acc.	categorical	−0.0228	−0.0095 \pm 0.0064	−0.0036
	numerical	−0.0276	−0.0108 \pm 0.0076	0.0005

by about .01 on average when compared to the uninterpretable, best-performing state-of-the-art models (XGBoost). Compared to CART, a different training process of the same model, slightly improves the accuracy, but importantly improves the minimum leaf accuracy, sometimes by up to 20 percentage points.

5 Conclusions and Limitations

We have identified an important problem of the *fairness* and *validity* of an explanation, and shown that contemporary tree-based models do leave room for improvement, in terms of fairness. The use of hybrid trees, where the top is constructed with the goal of maximizing minimum leaf accuracy, offers multiple benefits. First, it ensures better validity of every explanation provided, improving the minimum leaf accuracy by around 11 percentage points on average across the benchmark of tabular datasets [27]. Second, the extended accuracy with tree-based models suspended from leaves improves over the accuracy of low-depth trees constructed using integer programming as well as hybrid trees, where both top and bottom is obtained using CART. Finally, it is easy to extend to further constraints, such as shape constraints, in the top tree. Overall, we hope that the proposed approach may lead to improving the validity and fairness of decision trees as explanations.

The proposed approach shares some of the limitations of the original optimal decision trees [43]. Notably, the algorithms for solving mixed-integer program-

ming problems we utilize scale exponentially in the number of decision variables. Having said that, depth-4 trees suffice to match state-of-the-art methods in terms of accuracy when additional tree-based models are suspended from the leaves, which makes exponential time algorithms sufficiently fast in practice. Furthermore, all recently proposed methods [60, 61, 51, 62, 63, e.g.] improving the scalability of optimal decision trees can be applied, in principle.

References

- [1] H. J. Payne and W. S. Meisel, “An algorithm for constructing optimal binary decision trees,” *IEEE Transactions on Computers*, vol. C-26, pp. 905–916, 1977.
- [2] L. Breiman, J. Friedman, C. Stone, and R. Olshen, *Classification and Regression Trees*. Taylor & Francis, 1984.
- [3] E. Mays, *Handbook of credit scoring*. Global Professional Publishing, 1995.
- [4] L. Thomas, J. Crook, and D. Edelman, *Credit scoring and its applications*. SIAM, 2017.
- [5] S. Lessmann, B. Baesens, H.-V. Seow, and L. C. Thomas, “Benchmarking state-of-the-art classification algorithms for credit scoring: An update of research,” *European Journal of Operational Research*, vol. 247, no. 1, pp. 124–136, 2015.
- [6] S. Athey and G. W. Imbens, “Machine learning methods that economists should know about,” *Annual Review of Economics*, vol. 11, pp. 685–725, 2019.
- [7] “Equal Credit Opportunity Act (ECOA).” <https://www.law.cornell.edu/uscode/text/15/chapter-41/subchapter-IV>, 1974. Title 15 of the United States Code, Chapter 41, Subchapter IV, paragraph 1691 and following.
- [8] European Commission, “Directive 2013/36/EU of the European Parliament and of the Council of 26 june 2013 on access to the activity of credit institutions and the prudential supervision of credit institutions and investment firms, amending Directive 2002/87/EC and repealing Directives 2006/48/EC and 2006/49/ec.,” 2016. Accessed: 2023-04-30.
- [9] European Commission, “Regulation (EU) 2016/679 of the European Parliament and of the Council of 27 April 2016 on the protection of natural persons with regard to the processing of personal data and on the free movement of such data, and repealing Directive 95/46/EC (General Data Protection Regulation).,” 2016. Accessed: 2023-04-30.

- [10] C. Rudin, “Stop explaining black box machine learning models for high stakes decisions and use interpretable models instead,” *Nature Machine Intelligence*, vol. 1, no. 5, pp. 206–215, 2019.
- [11] P. Bracke, A. Datta, C. Jung, and S. Sen, “Machine learning explainability in finance: an application to default risk analysis.” Staff Working Paper No. 816 of the Bank of England, <https://www.bankofengland.co.uk/working-paper/2019/>, 2019. Accessed: 2023-04-30.
- [12] L. Dupont, O. Fliche, and S. Yang, “Governance of artificial intelligence in finance.” Discussion papers of Autorité de Contrôle Prudentiel et de Résolution, <https://acpr.banque-france.fr/en/governance-artificial-intelligence-finance>, 2020. Accessed: 2023-04-30.
- [13] Consumer Financial Protection Bureau, “Consumer financial protection circular 2022-03: Adverse action notification requirements in connection with credit decisions based on complex algorithms.” <https://www.consumerfinance.gov/compliance/circulars/>, 2022. Accessed: 2023-04-30.
- [14] B. R. Gunnarsson, S. Vanden Broucke, B. Baesens, M. Óskarsdóttir, and W. Lemahieu, “Deep learning for credit scoring: Do or don’t?,” *European Journal of Operational Research*, vol. 295, no. 1, pp. 292–305, 2021.
- [15] T. Brennan, W. Dieterich, and B. Ehret, “Evaluating the predictive validity of the compas risk and needs assessment system,” *Criminal Justice and behavior*, vol. 36, no. 1, pp. 21–40, 2009.
- [16] T. Brennan and W. Dieterich, *Correctional Offender Management Profiles for Alternative Sanctions (COMPAS)*, ch. 3, pp. 49–75. John Wiley & Sons, Ltd, 2018.
- [17] R. Courtland, “The bias detectives,” *Nature*, vol. 558, no. 7710, pp. 357–360, 2018.
- [18] Q. Zhou, J. Marecek, and R. N. Shorten, “Fairness in forecasting of observations of linear dynamical systems,” *Journal of AI Research*, vol. 76, pp. 1245–1280, 2023. arXiv preprint arXiv:2209.05274.
- [19] E. Rakha, D. Soria, A. R. Green, C. Lemetre, D. G. Powe, C. C. Nolan, J. M. Garibaldi, G. Ball, and I. O. Ellis, “Nottingham prognostic index plus (npi+): a modern clinical decision making tool in breast cancer,” *British journal of cancer*, vol. 110, no. 7, pp. 1688–1697, 2014.
- [20] A. J. London, “Artificial intelligence and black-box medical decisions: accuracy versus explainability,” *Hastings Center Report*, vol. 49, no. 1, pp. 15–21, 2019.

- [21] E. Tjoa and C. Guan, “A survey on explainable artificial intelligence (XAI): Toward medical XAI,” *IEEE transactions on neural networks and learning systems*, vol. 32, no. 11, pp. 4793–4813, 2020.
- [22] O. Bastani, C. Kim, and H. Bastani, “Interpreting blackbox models via model extraction,” *arXiv preprint arXiv:1705.08504*, 2017.
- [23] J. Feldman, “Minimization of boolean complexity in human concept learning,” *Nature*, vol. 407, no. 6804, pp. 630–633, 2000.
- [24] L. Wolf, T. Galanti, and T. Hazan, “A formal approach to explainability,” in *Proceedings of the 2019 AAAI/ACM Conference on AI, Ethics, and Society*, pp. 255–261, 2019.
- [25] J. Singh, M. Khosla, W. Zhenye, and A. Anand, “Extracting per query valid explanations for blackbox learning-to-rank models,” in *Proceedings of the 2021 ACM SIGIR International Conference on Theory of Information Retrieval*, pp. 203–210, 2021.
- [26] J. Marques-Silva and A. Ignatiev, “Delivering trustworthy ai through formal xai,” in *Proceedings of the AAAI Conference on Artificial Intelligence*, vol. 36, pp. 12342–12350, 2022.
- [27] L. Grinsztajn, E. Oyallon, and G. Varoquaux, “Why do tree-based models still outperform deep learning on typical tabular data?,” in *Thirty-sixth Conference on Neural Information Processing Systems Datasets and Benchmarks Track*, 2022.
- [28] Z.-H. Zhou and Z.-Q. Chen, “Hybrid decision tree,” *Knowledge-based systems*, vol. 15, no. 8, pp. 515–528, 2002.
- [29] L. Breiman, “Random forests,” *Machine learning*, vol. 45, pp. 5–32, 2001.
- [30] L. Mason, J. Baxter, P. Bartlett, and M. Frean, “Boosting algorithms as gradient descent,” *Advances in neural information processing systems*, vol. 12, 1999.
- [31] J. H. Friedman, “Greedy function approximation: A gradient boosting machine.,” *The Annals of Statistics*, vol. 29, no. 5, pp. 1189 – 1232, 2001.
- [32] S. Athey and G. Imbens, “Recursive partitioning for heterogeneous causal effects,” *Proceedings of the National Academy of Sciences*, vol. 113, no. 27, pp. 7353–7360, 2016.
- [33] A. B. Arrieta, N. Díaz-Rodríguez, J. Del Ser, A. Bennetot, S. Tabik, A. Barbado, S. García, S. Gil-López, D. Molina, R. Benjamins, *et al.*, “Explainable artificial intelligence (xai): Concepts, taxonomies, opportunities and challenges toward responsible ai,” *Information fusion*, vol. 58, pp. 82–115, 2020.

- [34] N. Burkart and M. F. Huber, “A survey on the explainability of supervised machine learning,” *Journal of Artificial Intelligence Research*, vol. 70, pp. 245–317, 2021.
- [35] C. Rudin, C. Chen, Z. Chen, H. Huang, L. Semenova, and C. Zhong, “Interpretable machine learning: Fundamental principles and 10 grand challenges,” *Statistic Surveys*, vol. 16, pp. 1–85, 2022.
- [36] H. Laurent and R. L. Rivest, “Constructing optimal binary decision trees is np-complete,” *Information processing letters*, vol. 5, no. 1, pp. 15–17, 1976.
- [37] X. Wu, V. Kumar, J. Ross Quinlan, J. Ghosh, Q. Yang, H. Motoda, G. J. McLachlan, A. Ng, B. Liu, P. S. Yu, *et al.*, “Top 10 algorithms in data mining,” *Knowledge and information systems*, vol. 14, pp. 1–37, 2008.
- [38] L. Breiman, “Arcing classifier (with discussion and a rejoinder by the author),” *The annals of statistics*, vol. 26, no. 3, pp. 801–849, 1998.
- [39] T. Chen and C. Guestrin, “Xgboost: A scalable tree boosting system,” in *Proceedings of the 22nd ACM SIGKDD International Conference on Knowledge Discovery and Data Mining*, KDD ’16, (New York, NY, USA), p. 785–794, Association for Computing Machinery, 2016.
- [40] G. Ke, Q. Meng, T. Finley, T. Wang, W. Chen, W. Ma, Q. Ye, and T.-Y. Liu, “Lightgbm: A highly efficient gradient boosting decision tree,” in *Advances in Neural Information Processing Systems* (I. Guyon, U. V. Luxburg, S. Bengio, H. Wallach, R. Fergus, S. Vishwanathan, and R. Garnett, eds.), vol. 30, Curran Associates, Inc., 2017.
- [41] L. Prokhorenkova, G. Gusev, A. Vorobev, A. V. Dorogush, and A. Gulin, “Catboost: unbiased boosting with categorical features,” *Advances in neural information processing systems*, vol. 31, 2018.
- [42] Y. Gorishniy, I. Rubachev, V. Khrulkov, and A. Babenko, “Revisiting deep learning models for tabular data,” in *Advances in Neural Information Processing Systems* (M. Ranzato, A. Beygelzimer, Y. Dauphin, P. Liang, and J. W. Vaughan, eds.), vol. 34, pp. 18932–18943, Curran Associates, Inc., 2021.
- [43] D. Bertsimas and J. Dunn, “Optimal classification trees,” *Machine Learning*, vol. 106, pp. 1039–1082, July 2017.
- [44] C. Bessiere, E. Hebrard, and B. O’Sullivan, “Minimising decision tree size as combinatorial optimisation,” in *Proceedings of the 15th International Conference on Principles and Practice of Constraint Programming*, CP’09, (Berlin, Heidelberg), p. 173–187, Springer-Verlag, 2009.
- [45] N. Narodytska, A. Ignatiev, F. Pereira, and J. Marques-Silva, “Learning optimal decision trees with sat,” in *Proceedings of the 27th International Joint Conference on Artificial Intelligence*, IJCAI’18, p. 1362–1368, AAAI Press, 2018.

[46] O. Günlük, J. Kalagnanam, M. Li, M. Menickelly, and K. Scheinberg, “Optimal decision trees for categorical data via integer programming,” *Journal of Global Optimization*, vol. 81, pp. 233–260, 2021. First appeared in a pre-print form in 2016 as arXiv:1612.03225.

[47] S. Verwer and Y. Zhang, “Learning optimal classification trees using a binary linear program formulation,” *Proceedings of the AAAI Conference on Artificial Intelligence*, vol. 33, pp. 1625–1632, Jul. 2019.

[48] X. Hu, C. Rudin, and M. Seltzer, “Optimal sparse decision trees,” *Advances in Neural Information Processing Systems*, vol. 32, 2019.

[49] R. Xin, C. Zhong, Z. Chen, T. Takagi, M. Seltzer, and C. Rudin, “Exploring the whole rashomon set of sparse decision trees,” *arXiv preprint arXiv:2209.08040*, 2022.

[50] R. Zhang, R. Xin, M. Seltzer, and C. Rudin, “Optimal sparse regression trees,” in *AAAI Conference on Artificial Intelligence (AAAI)*, 2023.

[51] J. van der Linden, M. de Weerdt, and E. Demirović, “Fair and optimal decision trees: A dynamic programming approach,” *Advances in Neural Information Processing Systems*, vol. 35, pp. 38899–38911, 2022.

[52] J. Lin, C. Zhong, D. Hu, C. Rudin, and M. Seltzer, “Generalized and scalable optimal sparse decision trees,” in *International Conference on Machine Learning*, pp. 6150–6160, PMLR, 2020.

[53] S. Dash, O. Gunluk, and D. Wei, “Boolean decision rules via column generation,” *Advances in neural information processing systems*, vol. 31, 2018.

[54] H. Zhu, P. Murali, D. Phan, L. Nguyen, and J. Kalagnanam, “A scalable mip-based method for learning optimal multivariate decision trees,” *Advances in neural information processing systems*, vol. 33, pp. 1771–1781, 2020.

[55] S. Aghaei, A. Gomez, and P. Vayanos, “Learning optimal classification trees: Strong max-flow formulations,” *arXiv preprint arXiv:2002.09142*, 2020.

[56] M. A. Carreira-Perpinán and P. Tavallali, “Alternating optimization of decision trees, with application to learning sparse oblique trees,” *Advances in neural information processing systems*, vol. 31, 2018.

[57] V. Zantedeschi, M. Kusner, and V. Niculae, “Learning binary decision trees by argmin differentiation,” in *International Conference on Machine Learning*, pp. 12298–12309, PMLR, 2021.

[58] E. Carrizosa, C. Molero-Rio, and D. Romero Morales, “Mathematical optimization in classification and regression trees,” *Top*, vol. 29, no. 1, pp. 5–33, 2021.

- [59] G. Nanfack, P. Temple, and B. Frénay, “Constraint enforcement on decision trees: A survey,” *ACM Comput. Surv.*, vol. 54, sep 2022.
- [60] T. Vidal and M. Schiffer, “Born-again tree ensembles,” in *Proceedings of the 37th International Conference on Machine Learning* (H. D. III and A. Singh, eds.), vol. 119 of *Proceedings of Machine Learning Research*, pp. 9743–9753, PMLR, 13–18 Jul 2020.
- [61] E. Demirović, A. Lukina, E. Hebrard, J. Chan, J. Bailey, C. Leckie, K. Ramamohanarao, and P. J. Stuckey, “Murtree: Optimal decision trees via dynamic programming and search,” *The Journal of Machine Learning Research*, vol. 23, no. 1, pp. 1169–1215, 2022.
- [62] K. Hua, J. Ren, and Y. Cao, “A scalable deterministic global optimization algorithm for training optimal decision tree,” *Advances in Neural Information Processing Systems*, vol. 35, pp. 8347–8359, 2022.
- [63] R. Mazumder, X. Meng, and H. Wang, “Quant-BnB: A scalable branch-and-bound method for optimal decision trees with continuous features,” in *Proceedings of the 39th International Conference on Machine Learning* (K. Chaudhuri, S. Jegelka, L. Song, C. Szepesvari, G. Niu, and S. Sabato, eds.), vol. 162 of *Proceedings of Machine Learning Research*, pp. 15255–15277, PMLR, 17–23 Jul 2022.

A Appendix

In the Supplementary material, we also provide the source code and complete results in .csv files along with a Jupyter notebook with example tests in Supplementary Material, which will be publicly available once the paper is accepted. We also tabulate the results of further tests performed and describe ablation analyses.

A.1 Datasets

We used the classification part of the data sets from the mid-sized tabular data created by [27]. The datasets, with their properties, are listed in Table 2. Training sets contained 80% of the total amount of samples truncated to at most 10,000 samples. This constraint affects 16 of the 23 total datasets, although some only marginally. The affected datasets have their number of samples in Table 2 in bold. The remaining 20% of samples were the testing dataset. In a 10-fold cross-validation, we used 10 random seeds that determined the train-test splits of each dataset.

Additionally, datasets are either categorical or numerical. Categorical are those that contain at least one categorical feature. Numerical datasets have no categorical features. Four numerical datasets are the same as categorical datasets, but with their categorical features removed (*covtype*, *default-of-credit-card-clients*, *electricity*, *eye_movements*). Only datasets without missing features and with sufficient complexity are included in the benchmark. For more details on the methodology of dataset selection, we refer to the original paper [27].

A.2 MIP formulation description

We provide Table 3 with short descriptions of the parameters and variables in the proposed formulation in Figure 4.

A.3 MIP Solver

We have utilized Gurobi optimizer as a MIP solver. Although the solver makes steady progress towards global optimality, the road there is lengthy. Figure 7b shows the progress of the MIP Gaps during the 8-hour optimization averaged over all datasets. For a detailed, per-dataset view, see Figure 8. We see that the solution is still improving, albeit rather slowly, after 8 hours. The narrowing of the MIP gap is achieved only by finding better feasible solutions. This lack of improvement of the objective bound might have been affected by our hyperparameter settings which focused on finding feasible solutions and heuristic search. However, tests with default parameters did not improve the best bound either.

Table 2: Listed classification datasets of the tabular benchmark. Train sets contained 80% of the total amount of samples truncated to at most 10 000 samples. 16 datasets affected by this have their number of samples in bold.

categorical datasets	# of samples	# of features	# of classes
albert	58252	31	2
compas-two-years	4966	11	2
covertype	423680	54	2
default-of-credit-card-clients	13272	21	2
electricity	38474	8	2
eye_movements	7608	23	2
road-safety	111762	32	2
numerical datasets	# of samples	# of features	# of classes
bank-marketing	10578	7	2
Bioresponse	3434	419	2
california	20634	8	2
covertype	566602	32	2
credit	16714	10	2
default-of-credit-card-clients	13272	20	2
Diabetes130US	71090	7	2
electricity	38474	7	2
eye_movements	7608	20	2
Higgs	940160	24	2
heloc	10000	22	2
house_16H	13488	16	2
jannis	57580	54	2
MagicTelescope	13376	10	2
MiniBooNE	72998	50	2
pol	10082	26	2

Table 3: Description of MIP symbols used in the proposed formulation in Figure 4. Parameter n refers to the number of samples, K is the number of classes, p is the number of features, and d is the depth of the tree.

	Symbol	Explanation	Size
Params	Y_{ik}	Equal 1 for true class of a sample	$n \times K$
	\mathbf{x}_i	Input samples	$n \times p$
	ϵ	Minimal change in feature values	p
	ϵ_{\max}	Maximal value of ϵ	1
	N_{\min}	Minimum of samples in a leaf	1
	\mathcal{T}_L	Set of leaf nodes	2^d
	\mathcal{T}_B	Set of decision (branching) nodes	$2^d - 1$
	$A_L(t)$	Ancestors of leaf t that decide left	$\leq d - 1$
	$A_R(t)$	Ancestors of leaf t that decide right	$\leq d - 1$
Variables	Q	Tree's leaf accuracy	1
	s_{it}	Accuracy potential of \mathbf{x}_i in leaf t	$n \times 2^d$
	S_{it}	Accuracy contribution of \mathbf{x}_i in leaf t	$n \times 2^d$
	r_t	Reference accuracy for $s_{:t}$	2^d
	z_{it}	Assignment of \mathbf{x}_i to leaf t	$n \times 2^d$
	l_t	Non-emptiness of leaf t	2^d
	c_{kt}	Assignment of class k to leaf t	$K \times 2^d$
	a_{jt}	1 if deciding on feature j in node t	$p \times (2^d - 1)$
	b_t	Decision threshold in node t	$2^d - 1$

Table 4: Detailed view of the differences in the accuracy between default Heuristics parameter and the proposed configuration (Heuristics = 0.8). A positive number means the accuracy advantage of the proposed hyperparameter configuration. We see absolute mean differences of comparable values. The negative difference in leaf accuracy on numerical datasets also has a higher standard deviation, suggesting a stronger influence by an outlier dataset. For a graphical representation of this data, see Figure 7a.

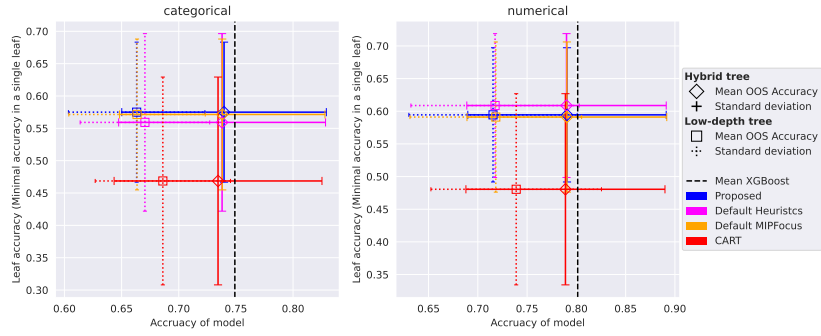
	Data type	Min	Mean (\pm std)	Max
Leaf Accuracy	categorical	-0.0117	0.0158 ± 0.0234	0.0531
	numerical	-0.1178	-0.0143 ± 0.0402	0.0435
Hybrid-tree Acc.	categorical	-0.0011	0.0017 ± 0.0035	0.0094
	numerical	-0.0047	0.0005 ± 0.0025	0.0062

A.3.1 Default hyperparameters of Gurobi solver

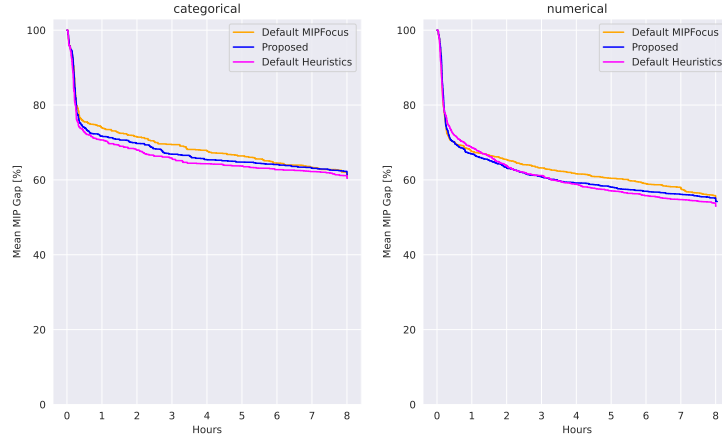
The performance of the Gurobi optimizer depends on the choice of hyperparameters. For the sake of simplicity, we have considered only two sets of parameters. To measure the performance change of our choice of (hyper)parameters, we ran a test with the default value of the MIPFocus parameter and a test with the default value of the Heuristics parameter.

The results (cf. Figure 7a and Tables 4, 5) show no significant improvements regarding the MIPFocus parameter. However, with the default value of the Heuristics parameter, we observe an improvement in performance on numerical datasets and a decrease in performance on categorical datasets. Both absolute differences in accuracy are about 0.015, so we opted for the variant with similar performances on both categorical and numerical datasets. That is the proposed variant focusing on heuristics. This proposed configuration also shows a more stable increase in accuracy w.r.t. the performance of CART models. The solver performance varies per dataset, as visualized by Figure 8.

These differences in performance suggest that hyperparameter space regarding the MIP solver should be further explored and could yield improvements. A closer look at Figure 8 suggests that different configurations help achieve better conditions for the solver on different datasets. This might be an area of further hyperparameter tuning based on the specific attributes of the dataset.



(a) Comparison of the Proposed model to models with default parameter configurations show varying results. MIPFocus seems to influence the search only very slightly. Heuristics, on the other hand, show significant improvement on numerical datasets and a decrease in performance on categorical datasets, with about the same absolute difference.



(b) Mean MIP optimality gap development over the solving time, averaged over all datasets. For a non-aggregated version, see Figure 8.

Figure 7: Comparison of models with the proposed configuration of Gurobi hyperparameters and runs with default values of the modified parameters.

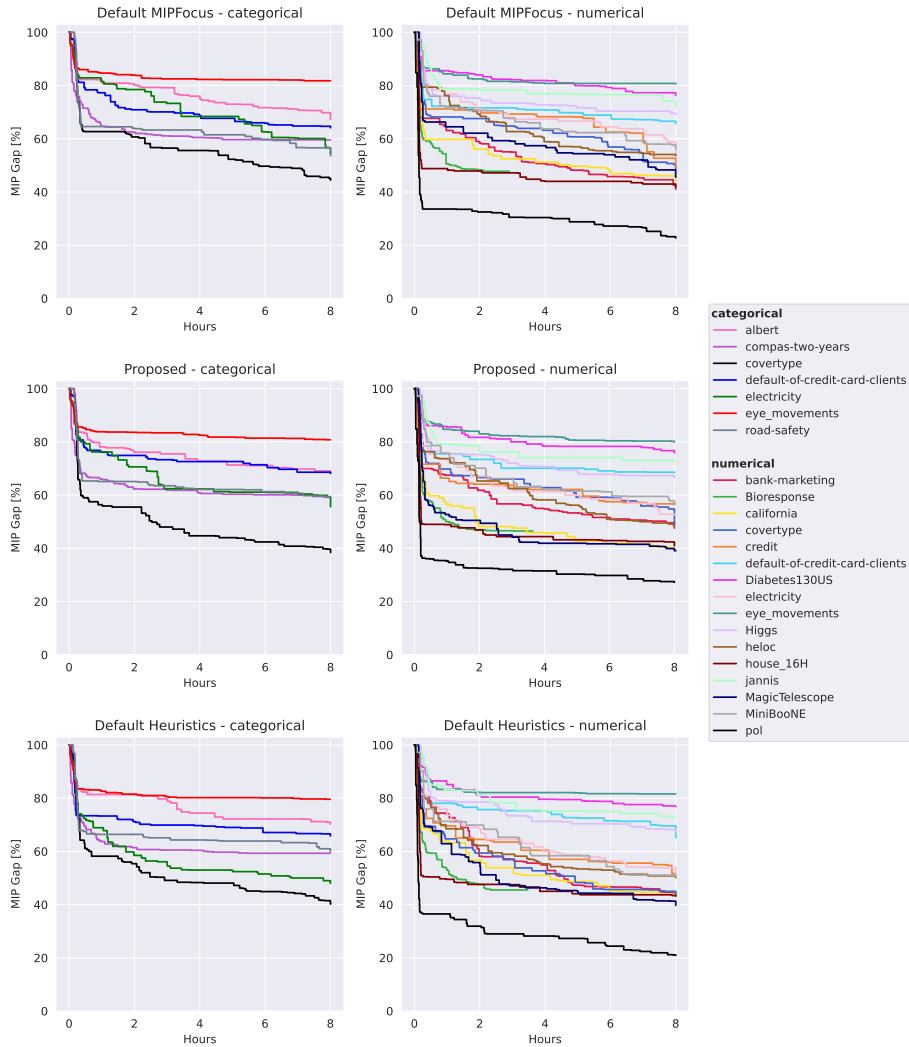


Figure 8: Mean MIP optimality gap development over the solving time, averaged over 10 different data splits. The figure shows the progress of the value of the MIP optimality gap averaged over all splits of each dataset. Each line corresponds to one dataset. For an aggregated version, see Figure 7b

Table 5: Detailed view of the differences in the accuracy between default MIP-Focus parameter and the proposed configuration (MIPFocus = 1). A positive number means the accuracy advantage of the proposed hyperparameter configuration. Both variants seem to perform comparably, with a potential slight edge in favor of the proposed configuration. For a graphical representation of this data, see Figure 7a.

	Data type	Min	Mean (\pm std)	Max
Leaf Accuracy	categorical	−0.0304	0.0036 \pm 0.0213	0.0299
	numerical	−0.0528	0.0034 \pm 0.0342	0.0788
Hybrid-tree Acc.	categorical	−0.0028	0.0016 \pm 0.0043	0.0088
	numerical	−0.0026	0.0001 \pm 0.0019	0.0032

A.4 Memory requirements

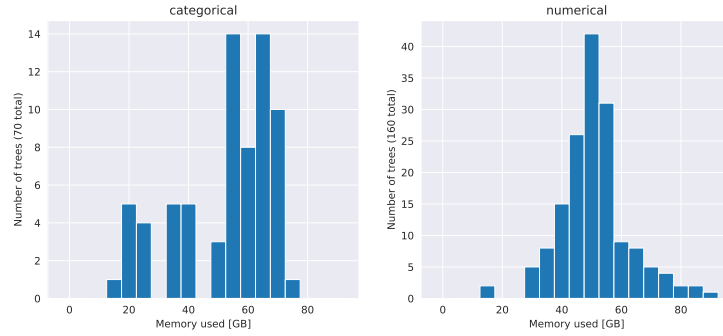
Overall, the memory requirements of the datasets were between 15 and 95 GB. On average, all datasets required at most 70 GB of working memory. Figure 9 shows the memory requirements of our formulation in more detail. The extension phase of the process is negligible in this regard, as it requires only about 1.5 GB of working memory in total and is performed after the MIP optimization. Training and extending the CART models also required less than 2 GB of working memory.

The amount of memory required by the MIP solver is dependent on the size of the data in the number of training samples, as well as the number of features. Figure 9b shows this linear dependence of memory requirements on the size of the training set. Based on the coloring of the nodes, we also see the dependence on the number of features, especially in the case of the Bioresponse dataset.

A.4.1 Performance of the model given a shorter time

When considering a shorter time for optimization, we can lower the memory requirements to levels attainable by current personal computers. When optimizing our MIP model for one hour, the required memory is below 50 GB for all datasets except Bioresponse, which has one order of magnitude more features than the rest of the datasets included in the benchmark. The mean memory requirement is below 30 GB of working memory (compared to 50 GB for the 8-hour run). See Figure 10 for details.

Figure 10c shows that even with this limited budget, we can achieve significant improvement compared to CART in leaf accuracy and similar accuracy of hybrid trees.

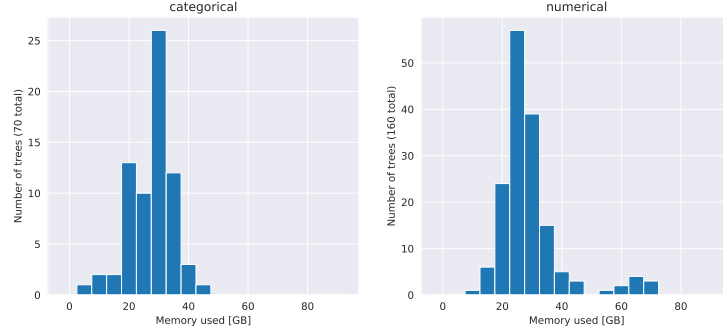


(a) Histogram of memory requirements of MIP solver for all dataset splits.



(b) Mean memory requirements on datasets. Dots are colored according to the number of features. Dataset Biorep is excluded from the color mapping due to having significantly more features. Training sets were truncated to a maximum of 10,000 points.

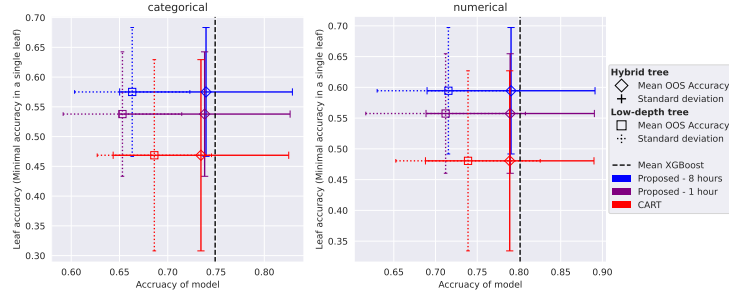
Figure 9: Memory requirements mostly do not exceed 70 GB. The memory requirements increase slightly when more time is given to the solver and significantly increase when bigger training sets are considered. We can also see some correlation between the number of features and memory requirements when looking at same-size datasets.



(a) Histogram of memory requirements of MIP solver for all dataset splits.



(b) Mean memory requirements on datasets. Dots are colored according to the number of features. Dataset Bioresponse is excluded from the color mapping due to having a significantly higher number of features. Training sets were clipped to a maximum of 10,000 points.



(c) Comparison of the performance of the Proposed model after 1 and 8 hours of optimization.

Figure 10: Comparison to a version of the Proposed model that the Gurobi solver optimized for only one hour. Compared to the main configuration, which ran for 8 hours, we notice a significant decrease in memory requirements for most datasets, up to tens of gigabytes.

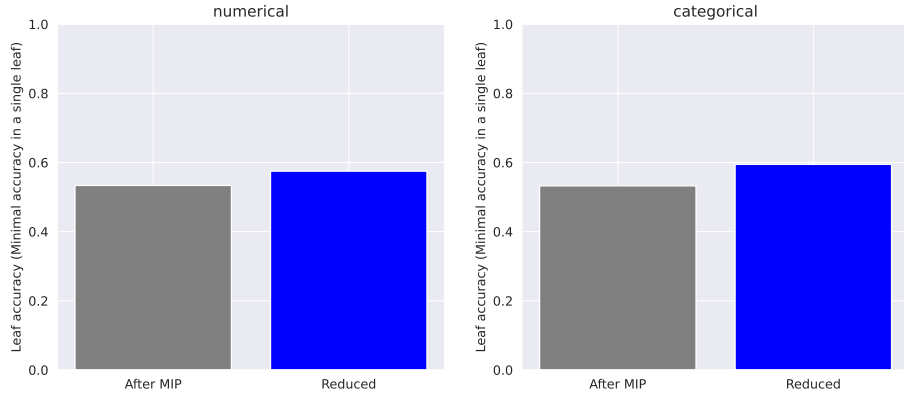


Figure 11: Effect of reduction on leaf accuracy of the model. In grey is the leaf accuracy before reduction, and in blue is the leaf accuracy after reduction. The plot shows mean accuracy over all datasets of a given type created by the proposed model.

A.5 Reduction of the trees

The reduction phase has a beneficial influence on the leaf accuracy of a model. Figure 11 shows this improvement of mean leaf accuracy over all datasets.

In Figure 12, we further provide a comparison of the complexity of the created trees by comparing the distributions of the number of leaves (or potential explanations) provided by the method.

The maximum amount of leaves of a tree with depth 4 is 16. CART model has, on average, around 8 leaves after reduction. Our proposed model’s distribution is close to the distribution of CART models. When solving the MIP formulation directly, the distribution is severely shifted toward very small trees. Our proposed method uses a default CART solution to warmstart the search, which might explain the shape of the distribution compared to the direct method and CART.

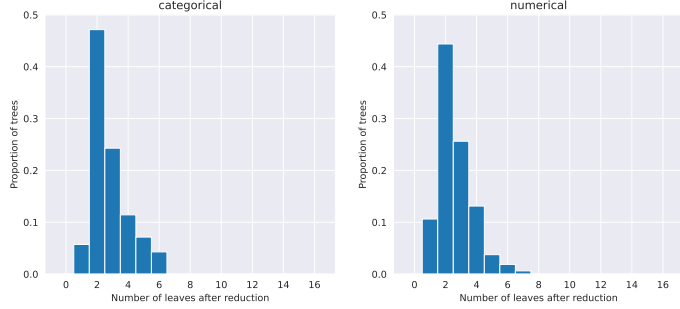
A.6 Hyperparameter search distributions

We needed to optimize hyperparameters for extending models and CART trees used for comparisons. We used Bayesian hyperparameter search for that purpose.

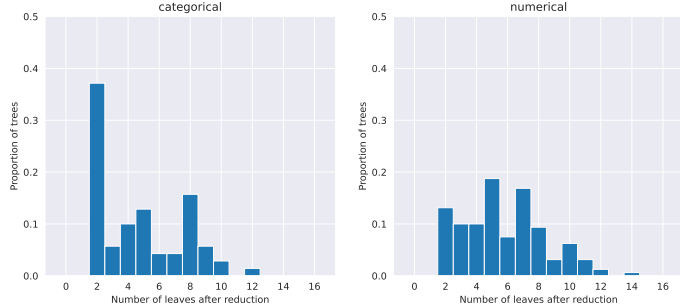
A.6.1 Extending XGBoost models

For the hyperparameter search of XGBoost models in leaves, we used the distributions listed in Table 6. The parameters are almost all the same as used by [27]. Only the Number of estimators and Max depth were more constrained to account for the fewer samples available for training.

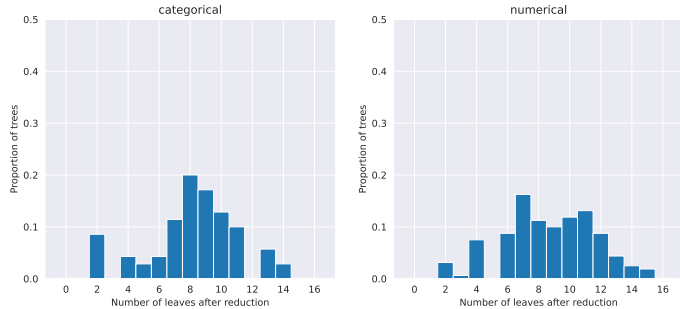
The Bayesian optimization was run for 50 iterations, with 3-fold cross-validation in every leaf that contained enough points to perform the optimization.



(a) Histogram of the number of leaves of the reduced trees optimized directly using the proposed formulation. The trees are heavily pruned.



(b) Histogram of the number of leaves of the reduced trees created with the proposed formulation, warmstarted using a simple CART solution. The trees are smaller compared to well-optimized CART but retain some complexity. This was the chosen method.



(c) Histogram of the number of leaves of the reduced trees created by CART with optimized hyperparameters.

Figure 12: Comparison of the numbers of leaves of trees after the reduction procedure.

Table 6: Distributions of hyperparameters of extending XGBoost models in leaves. These were used in the Bayesian hyperparameter search in each leaf separately. All distributions except Max depth and Number of estimators are the same as in [27]. The two different distributions were selected smaller to improve the optimization time and to account for lower amounts of data.

Parameter name	Distribution [range (inclusive)]
Max depth	UniformInteger [1, 7]
Number of estimators	UniformInteger [10, 500]
Min child weight	LogUniformInteger [1, 1e2]
Learning rate	Uniform [1e-5, 0.7]
Subsample	Uniform [0.5, 1]
Col sample by level	Uniform [0.5, 1]
Col sample by tree	Uniform [0.5, 1]
Gamma	LogUniform [1e-8, 7]
Alpha	LogUniform [1e-8, 1e2]
Lambda	LogUniform [1, 4]

Table 7: Distributions of hyperparameters of CART models used to compare to our method.

Parameter name	Distribution [range (inclusive)]
Max depth	UniformInteger [2, 4]
Min samples split	UniformInteger [2, 60]
Min samples leaf	UniformInteger [1, 60]
Max leaf nodes	UniformInteger [8, 16]
Min impurity decrease	Uniform [0, 0.2]

The same process was used to extend all tested trees.

In leaves with an insufficient amount of samples to perform the cross-validation (less than 3 samples of at least one class in our case), we train an XGBoost model with a single tree of max depth 5. In leaves with 100% training accuracy, we do not learn any model, and use the majority class.

A.6.2 CART models

For the hyperparameter optimization of CART models, we also used Bayesian search, with the distributions shown in the table 7.

The search was run for 100 iterations, with 5-fold cross-validation on the same training data sets as our model. After this search, the best hyperparameters were used to train the model on the full training data. The resulting tree was reduced and every leaf was extended by an XGBoost model in the same way as our models.

In comparisons in later Section A.9.1, we optimized a deeper variant of the CART. The process was the same, except for initial distributions of hyperparameters for Max depth and Max leaf nodes. Those were UniformInteger [2, 20] and UniformInteger [8, 512] respectively.

A.7 Detailed results

We also provide the full results for each dataset. Figures 13 and 14 are decomposed variants of Figure 5 for categorical and numerical datasets respectively. We also provide exact results, in Tables 8 and 9 respectively. The detailed results show that the proposed model outperforms the CART model in both accuracy measures on almost all datasets and has comparable accuracy to XGBoost.

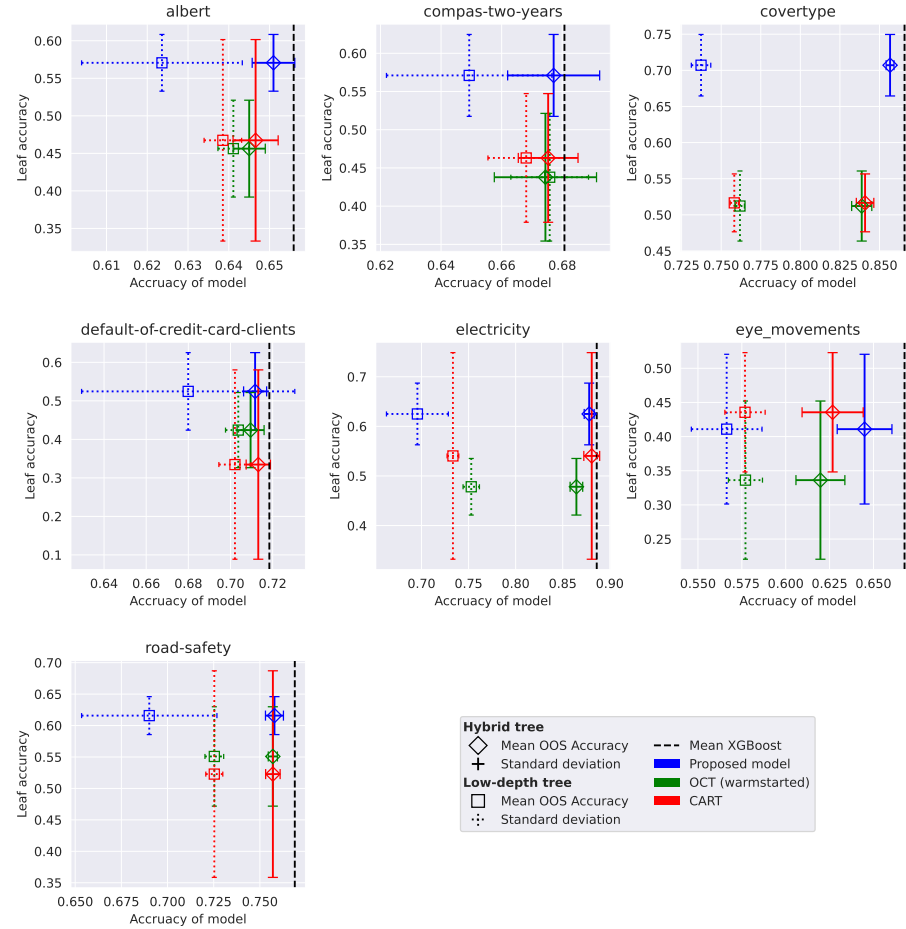


Figure 13: Detailed performance comparison of our model on categorical datasets.

Table 8: Categorical datasets. Mean accuracy of models on out-of-sample data and average ranks.

categorical	Leaf Accuracy		Hybrid-tree Acc.		
	CART	Proposed	CART	Proposed	XGBoost
albert	0.4674	0.5706	0.6466	0.6510	0.6559
compas-two-years	0.4631	0.5711	0.6754	0.6772	0.6807
covertype	0.5166	0.7071	0.8409	0.8567	0.8658
default-of-credit- -card-clients	0.3346	0.5246	0.7132	0.7117	0.7184
electricity	0.5404	0.6250	0.8808	0.8781	0.8861
eye_movements	0.4356	0.4109	0.6267	0.6449	0.6677
road-safety	0.5228	0.6158	0.7570	0.7579	0.7689
Mean rank	1.8571	1.1429	2.7143	2.2857	1.0000

Table 9: Numerical datasets. Mean accuracy of models on out-of-sample data and average ranks.

numerical	Leaf Accuracy		Hybrid-tree Acc.		
	CART	Proposed	CART	Proposed	XGBoost
bank-marketing	0.4083	0.5837	0.8011	0.8003	0.8044
Bioresponse	0.4738	0.5700	0.7655	0.7755	0.7920
california	0.5538	0.6861	0.8803	0.8914	0.8997
covertype	0.5391	0.6314	0.8094	0.8147	0.8190
credit	0.5153	0.6439	0.7715	0.7462	0.7738
default-of-credit- -card-clients	0.3422	0.5136	0.7118	0.7124	0.7156
Diabetes130US	0.4057	0.5204	0.6030	0.6051	0.6059
electricity	0.5404	0.6331	0.8692	0.8600	0.8683
eye_movements	0.4819	0.4265	0.6311	0.6364	0.6554
Higgs	0.4953	0.5698	0.6945	0.6992	0.7142
heloc	0.4909	0.6722	0.7106	0.7188	0.7183
house_16H	0.4985	0.6336	0.8702	0.8726	0.8881
jannis	0.4617	0.5079	0.7578	0.7632	0.7778
MagicTelescope	0.4719	0.6835	0.8481	0.8518	0.8605
MiniBooNE	0.4420	0.5809	0.9184	0.9194	0.9369
pol	0.5680	0.6550	0.9804	0.9811	0.9915
Mean rank	1.9375	1.0625	2.7500	2.1250	1.1250

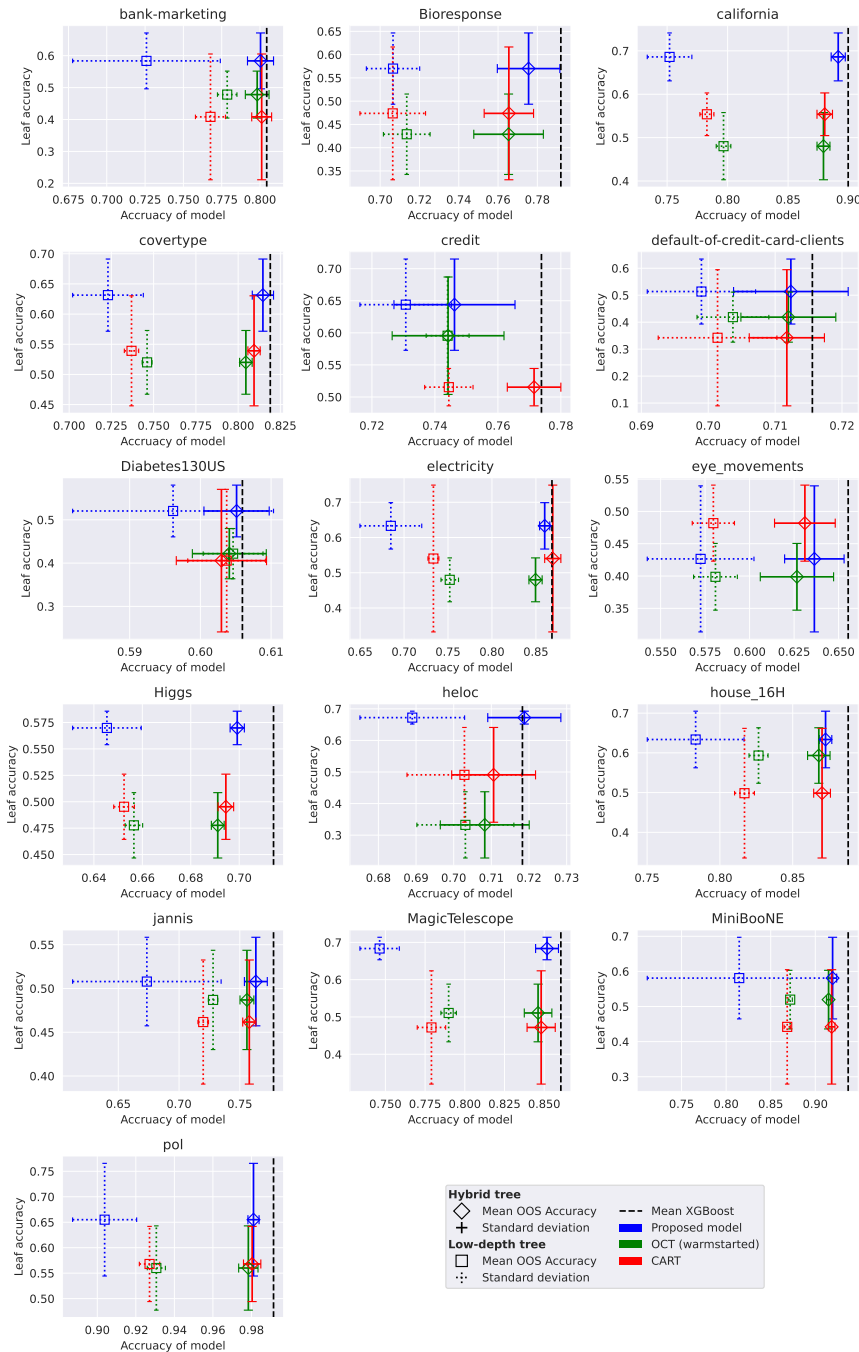


Figure 14: Detailed performance comparison of our model on numerical datasets

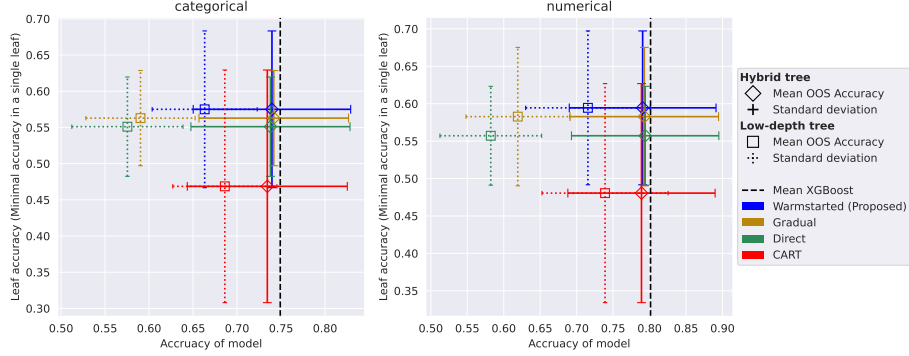


Figure 15: Comparison of the various approaches to the optimization given the same resources and conditions. Warmstarted refers to the approach of starting the optimization process with a CART solution. The gradual approach is the approach of increasing the depth of a tree and starting each new depth with the solution of the previous, shallower tree. Direct means a simple, straightforward optimization of the formulation as it is stated, without any hints. All three approaches were run with the same resources. For a closer investigation of the Gradual approach see Table 10.

A.8 Other optimization approaches

The best-performing approach of warmstarting the MIP solver with a CART solution is not the only one we tested. In Figure 15, we see a comparison of three different approaches to optimization.

- *Direct* refers to the straightforward use of the MIP formulation.
- *Warmstarted* uses a simple CART solution (created using default hyperparameters) as a starting point of the solving process.
- *Gradual* refers to a special process where we start by training a tree with a depth equal to 1 and use the solution found in some given time to start the search for a tree with a depth of 2 and so forth until we reach the desired depth.

All of the three approaches were run with the same resources. This meant that even the gradual approach took 8 hours in total. The time was distributed in a way that the available time for the optimization process doubled with each increase in depth. This means 32 minutes for the first run, 64 minutes for the tree of depth 2, 128 for depth 3, and 4 hours 16 minutes for the final tree with depth 4.

Interestingly, while the direct approach understandably does not reach a performance similar to the warmstarted variant, the gradual approach shows more promise. It has higher hybrid-tree accuracy by another 0.2 percentage

Table 10: Comparison of Gradual and Warmstarted approach. Positive numbers show an advantage in the mean accuracy of the Proposed (Warmstarted) approach. Gradual refers to the approach when the depth of the tree is gradually increased during the optimization process.

	Data type	Min	Mean (\pm std)	Max
Leaf Accuracy	categorical	-0.1094	0.0122 ± 0.0753	0.1130
	numerical	-0.0867	0.0117 ± 0.0624	0.1154
Hybrid-tree Acc.	categorical	-0.0219	-0.0021 ± 0.0094	0.0083
	numerical	-0.0103	-0.0023 ± 0.0056	0.0076

points on average while having lower leaf accuracy by about 1.2 percentage points compared to the warmstarted approach (cf. Table 10).

A.9 Ablation Analyses

We provide some comparing experiments performed by changing a single hyperparameter and 2 closely related hyperparameters, in the case of CART depth.

A.9.1 Unlimited depth CART

An argument could be made against our choice to compare our method to CART trees with the same limit on depth. Figure 16 and Table 11 in more detail show a comparison of CART models with a maximal depth of 4 and a maximal depth of 20. The actual depth limit for each model was optimized along with other hyperparameters using the Bayes hyperparameter optimization procedure. More details

The aggregated results show worse performance regarding both leaf accuracy and hybrid-tree accuracy. Not only do the deeper trees perform worse, but the length of provided explanations is also well above the 5-9 threshold suggested as the limit of human understanding [23].

Table 11: Detailed view of the differences in the accuracy between CART trees with max depth 4 and CART trees with max depth 20. A positive number means the accuracy advantage of the more constrained model (depth ≤ 4). For a graphical representation, see Figure 16

	Data type	Min	Mean (\pm std)	Max
Leaf Accuracy	categorical	-0.0769	0.2053 ± 0.2389	0.5404
	numerical	-0.1183	0.2441 ± 0.2115	0.5680
Hybrid-tree Acc.	categorical	-0.0025	0.0173 ± 0.0185	0.0420
	numerical	-0.0006	0.0156 ± 0.0119	0.0370

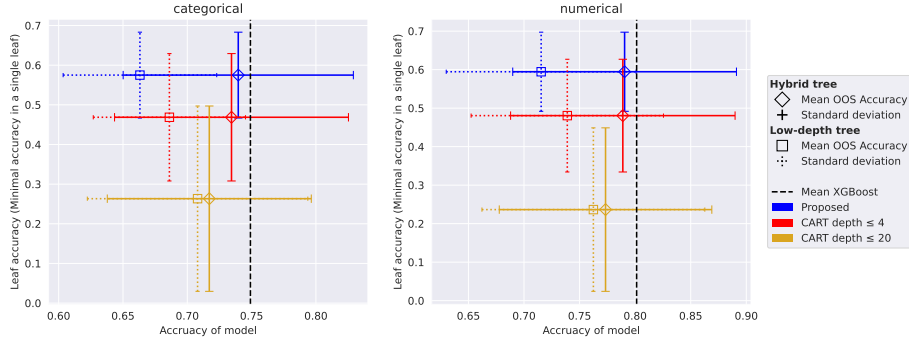


Figure 16: Comparison of CART tree results with limited depth and without such a strict limit on the depth. Deeper trees provide worse explanations (due to the length of explanation) and perform worse in both accuracy measures. For a more detailed description of the differences introduced by the depth, consult Table 11

A.9.2 Non-warmstarted OCT

We compare our method to warmstarted OCT because both start from the same CART initial solution. This makes them more comparable. However, we also tested the OCT variant, directly optimized from the MIP formulation. See the results in Figure 17. Both OCT models were run with the same hyperparameters as the proposed model. Those being heuristics-oriented solver, depth equal to 4, and a minimal amount of samples in leaves equal to 50.

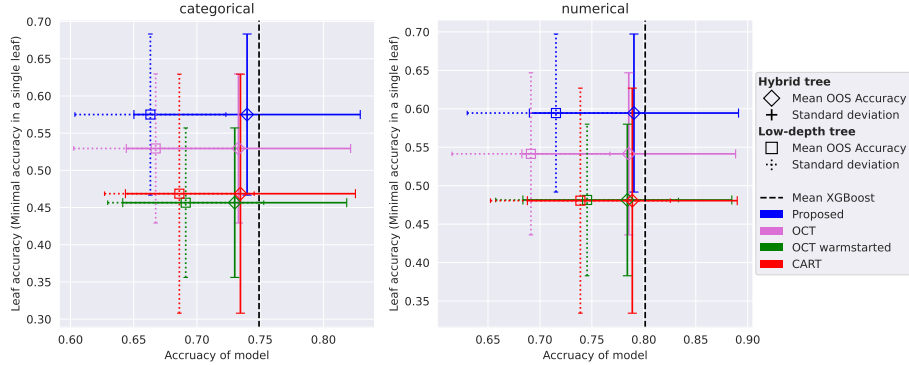
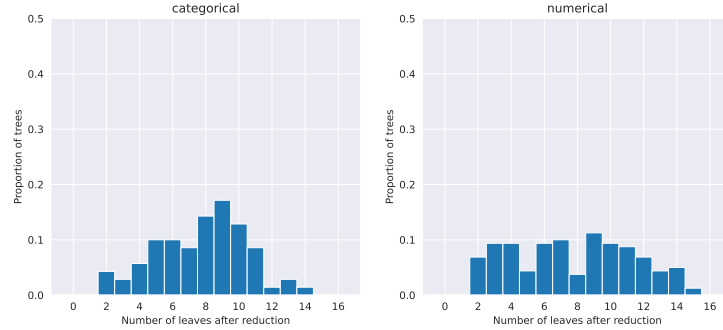
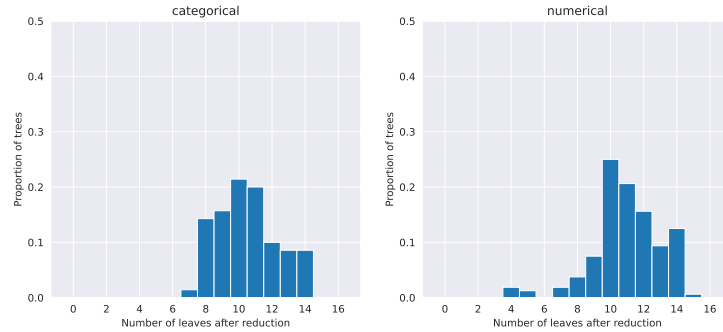


Figure 17: Comparison of OCT trees that are warmstarted the same way as our Proposed model and OCT without the warmstart, optimized directly. Interestingly, direct OCT performs significantly better.

The average OCT performs worse than all our approaches (cf. Figure 15), but the improvement from the warmstarted variant is intriguing. Especially



(a) Histogram of the number of leaves in the reduced trees of the direct OCT method



(b) Histogram of the number of leaves in the reduced trees of the warmstarted OCT method.

Figure 18: Comparison of reduced tree complexity of the OCT with and without warmstart. OCT without warmstart creates trees of similar distribution as the CART method (cf. Figure 12). And it achieves better leaf accuracy than CART (cf. Figure 17) despite neither optimizing that objective.

considering that it is not caused by the direct OCT method's inability to create complex trees without warmstarting. This is supported by Figure 18 showing a distribution of leaves similar to the distribution of CART trees (cf. Figure 12). This suggests that the OCT trees have comparable tree complexity to CART and provide more valid explanations than CART, even without our extension to the formulation. This is an interesting result, considering the fact that neither CART nor OCT methods optimize for leaf accuracy.

Our model, however, almost doubles the improvement of direct OCT. Its improvement is similar in the number of percentage points to OCT's improvement on CART.

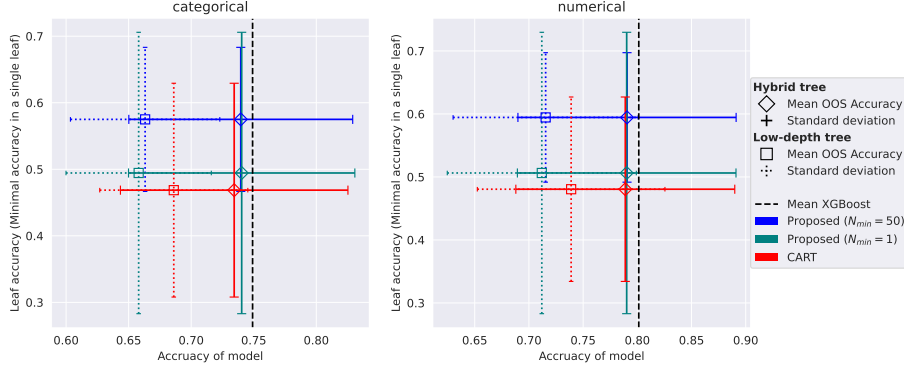


Figure 19: Comparison of performance of the proposed model with minimum samples in leaves equal 50 and 1. Lack of constraint leads to overfitting to training data and worse out-of-sample performance. Notice the high deviation of the model with $N_{min} = 1$. CART’s minimal amount of samples in leaves was optimized in hyperparameter search, according to Table 7.

A.9.3 No minimum number of samples in leaves

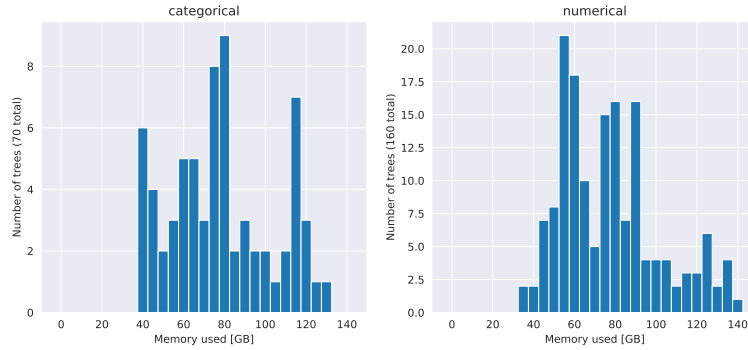
This comparison, see Figure 19, shows the importance of setting a minimal amount of samples in leaves. Without enough points to support the leaf’s accuracy, it is more likely to be overfitted. On the other hand, when choosing the N_{min} parameter too high, we restrict some possibly beneficial splits, supported by a smaller amount of training data.

N_{min} is a critical hyperparameter, and further testing could provide more insight into the proposed model’s performance.

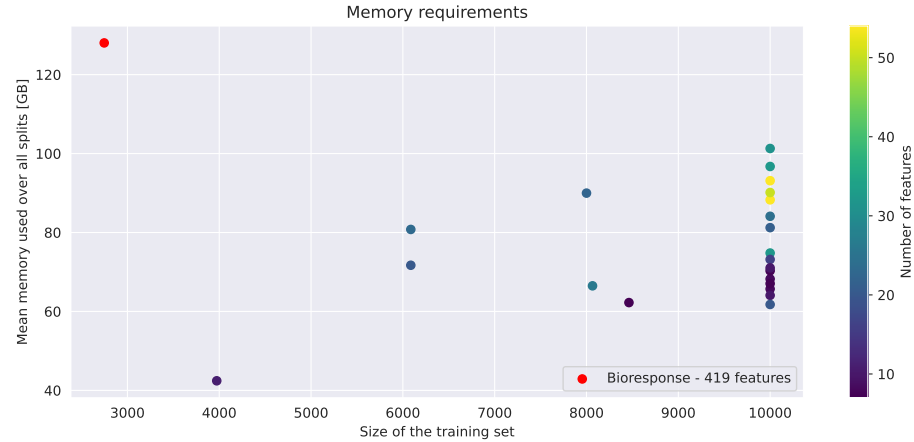
A.9.4 Deeper trees

Lastly, we provide a comparison of the proposed model of depths 4 and 5. Figure 21 shows better overall results for shallower trees. This is likely caused by the exponential increase in memory requirements, given the decrease in overall accuracy as well. We provide data about its memory usage in Figure 20. With a model of twice the complexity, the solver struggles to achieve comparable results to the shallower proposed model.

This is certainly a topic of further exploration by incorporating scalability improvements proposed in the literature.



(a) Depth 5. Histogram of memory requirements of MIP solver for all dataset splits.



(b) Depth 5. Mean memory requirements on datasets. Dots are colored according to the number of features. Dataset Bioresponse is excluded from the color mapping due to having a significantly higher number of features. Training sets were clipped to a maximum of 10,000 points.

Figure 20: Comparison of the memory requirements of the Proposed model with depth 5. The mean memory requirement almost increases from cca 51.1 GB to 77.3 GB with an increase in depth from 4 to 5. Compare the above plots with Figure 9

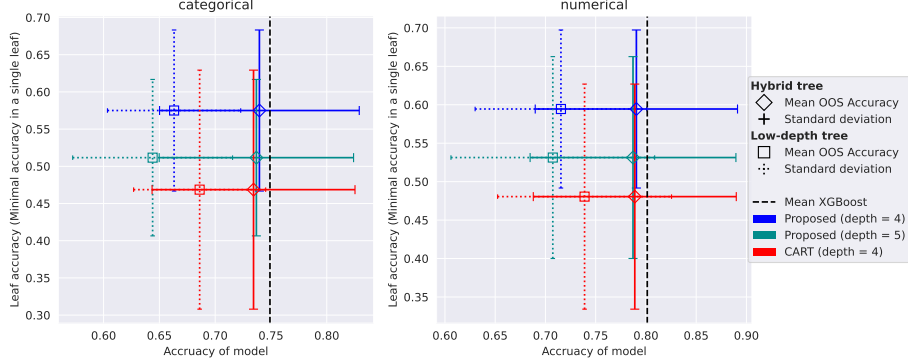


Figure 21: Comparison of performances of the proposed model with depths 4 and 5. Shallower trees perform better, possibly because they are easier to optimize.

A.10 Fixed hyperparameters CART

We compare our model to a CART model with optimized hyperparameters, as is common in practice. However, suppose we exclude the depth and minimum of samples in a leaf from the optimization and set them to reflect our settings for the proposed model. In that case, we achieve improved accuracy of the CART models as visualized in Figure 22 and expressed more clearly in Table 12. The proposed model still performs significantly better, by 6 to 8 percentage points in leaf accuracy, with maxima at 18 percentage points.³

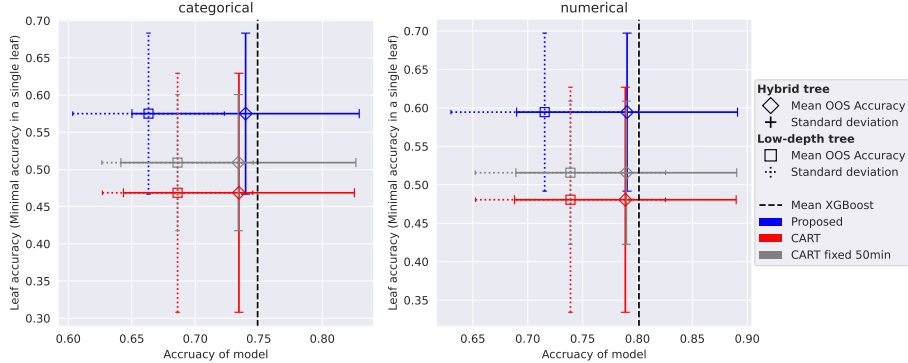


Figure 22: Comparison of CART trees with hyperparameters trained in full as described in the paper (in red) and CART trees with fixed hyperparameters of depth (4) and a minimum of samples in leaves (50) in grey.

³These results were obtained after the Paper Submission Deadline. That is why they are not presented in the main body of the paper.

Table 12: Detailed view of the differences in the accuracy between our model and CART with fixed depth and the minimum samples in leaf parameters. A positive number means the accuracy advantage of the proposed model (depth ≤ 4). For a graphical representation, see Figure 22

	Data type	Min	Mean (\pm std)	Max
Leaf Accuracy	categorical	-0.0321	0.0658 ± 0.0686	0.1813
	numerical	0.0036	0.0788 ± 0.0478	0.1641
Hybrid-tree Acc.	categorical	-0.0046	0.0057 ± 0.0083	0.0186
	numerical	-0.0244	0.0007 ± 0.0078	0.0100

A.11 More data

The 10,000 size limit on training samples was suggested by the authors of the benchmark [27]. Another good reason for such a limit is that we want our model to balance the size of the formulation and the capability of the formulated model. In other words, if we take a small amount of data, we are less likely to grasp the intricacies of the target variable distribution within the dataset. And if we take too many samples, we create a formulation that will not achieve good performance in a reasonable time.

In a comparison of a model learned on a training dataset limited to 10,000 samples with a dataset limited to 50,000 samples, we see that more data does not necessarily lead to a better model, given same time resources, see Figure 23. The 50,000 model is worse because of the too-demanding complexity of the formulation.

It improves the model accuracy, which is unsurprising since each leaf obtains more samples. The comparison to XGBoost is unreliable since the mean value for XGBoost was computed from the performance of models trained on at most 10,000 samples.

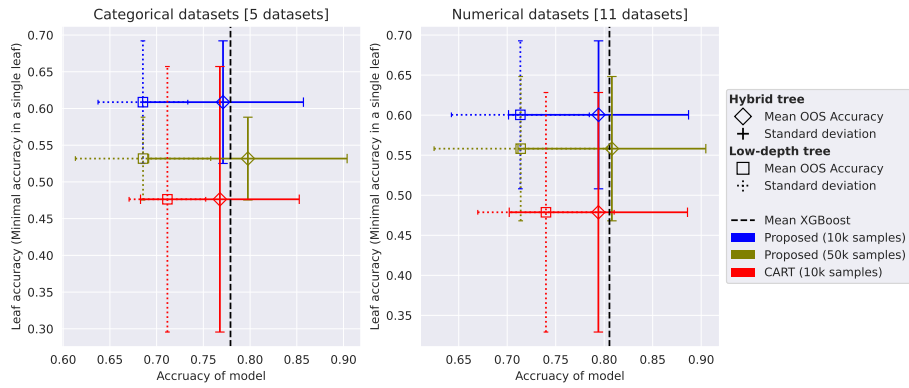


Figure 23: Comparison of a proposed model trained on at most 10,000 and 50,000 data samples. We use only datasets where the constraint caused a change, meaning that we omit datasets with less than 12,500 samples. The number of datasets is in square brackets. All other presented models use only 10,000 samples, so the comparison of model accuracies is not fully representative.